C. T.-C. Nguyen and R. T. Howe, "Polysilicon microresonators for signal processing," Digest of Papers, Government Microcircuit and Applications Conference, San Diego, CA, Aug. 15, 1994, pp. 195-198.

POLYSILICON MICRORESONATORS FOR SIGNAL PROCESSING

Clark T.-C. Nguyen and Roger T. Howe

Berkeley Sensor & Actuator Center
Department of Electrical Engineering and Computer Sciences
and the Electronics Research Laboratory
University of California at Berkeley
Berkeley, California 94720

Abstract

Completely monolithic micromechanical signal processors constructed of polycrystalline silicon are described. A high-Q oscillator, fabricated via a combined CMOS plus surface micromachining technology, is detailed, for which the oscillation frequency is controlled by a polysilicon micromechanical resonator to achieve high stability. High-Q electronic filters based upon micromechanical biquad stages and spring-coupled resonators are also presented. Brownian motion and mass loading phenomena are shown to have a greater influence on short-term frequency stability in this micro-scale.

Introduction

Mechanically-based components are widely used in communication circuits for high-Q filtering at the IF and RF frequencies and to generate precision local oscillators. Among the most commonly used mechanical devices are quartz crystals and SAW filters, which are off-chip components that interface with signal processing circuitry at the board level. The current trend to include increasing amounts of a total system on a single silicon chip makes fully monolithic high-Q filters and oscillators, where the mechanical element is fabricated on-chip, desirable.

Such an oscillator has recently been demonstrated [1,2], which utilizes a surface-micromachined, polycrystalline silicon resonator [3] frequency-setting element and CMOS electronics to sustain oscillation, all fabricated onto a single silicon chip (Fig. 1). The cross-section of the combined CMOS plus surface micromachining technology used to fabricate this oscillator [1,2,4] is shown in Fig. 2. Passive filters, without on-chip electronics, have also been demonstrated

With Q's of over 80,000 [5] under vacuum and center frequency temperature coefficients in the range of -10 ppm/°C (several times less with nulling techniques) [6], polysilicon micromechanical resonators can serve reasonably well as miniaturized substitutes for crystals in a variety of high-Q oscillator and filtering applications. This paper presents several specific examples of micromechanics applied to the processing of electronic signals.

Resonator Design

To simplify the task of integrating CMOS with micromechanics, capacitive excitation and detection is utilized for the µresonators in this work. A variety of capacitive topologies are available in this technology, and each will dictate the frequency tuning range and stability of the µresonator.

Figure 3 shows the cross-section of a parallel-plate capacitively driven µcantilever resonator in a typical bias and excitation configuration [8]. Here, an ac voltage v_i electrostatically drives the cantilever. The dc-bias voltage V_P amplifies the resulting force components at the frequency of v_i and sources the output motional current. In this scheme, the beam-to-electrode capacitance is nonlinearly dependent upon beam displacement, i.e., the change in capacitance vs. displacement, $\partial C/\partial x$, is a strong function of displacement. This leads to an electrical spring constant, $k_e = V_P^2 (C_o/d^2)$, which subtracts from the mechanical spring constant k_m and makes the center frequency f_o a function of the dc-bias voltage V_P [7,1]. This provides a convenient means for voltage control of the center frequency, making parallel-plate driven resonators useful for VCO applications. A -3600 ppm/V fractional frequency change is typical for a 20 kHz µresonator with a nominal V_P=10 V. However, the above also suggests that oscillators referenced to parallel-plate capacitively driven µresonators are less stable against power supply variations, due to electronic noise or temperature.

To eliminate this component of frequency instability, the electrode-to-resonator capacitance must be made to vary linearly with resonator displacement. In this work, this is achieved by using interdigitated-comb finger drive and sense capacitors [3]. Figure 4 shows a µresonator which utilizes interdigitated-

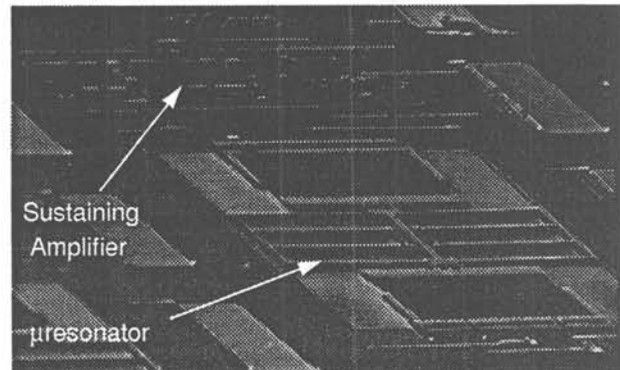

Fig. 1:SEM of the integrated CMOS µresonator oscillator.

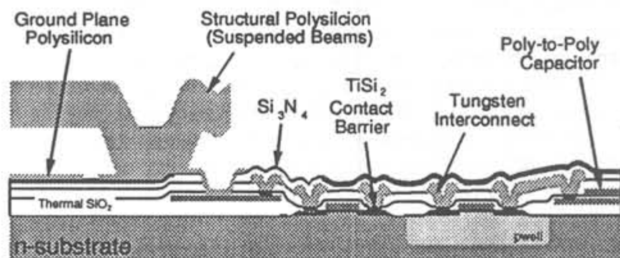

Fig. 2:Cross-section of the MICS technology for integration of CMOS and microstructures.

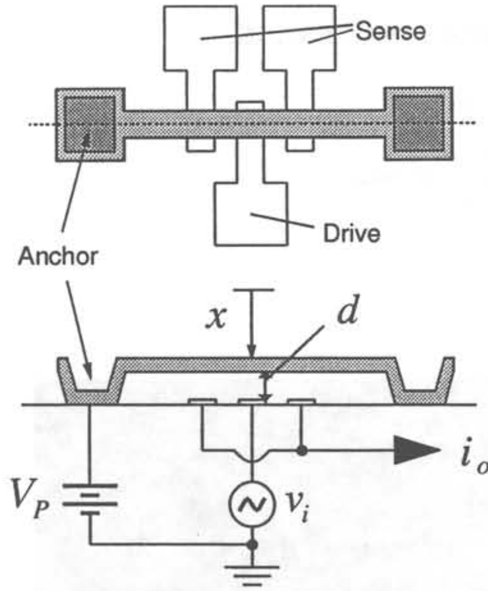

Fig. 3: Overhead and cross-sectional view of a vertical parallel-plate capacitively driven resonator with typical applied bias and excitation voltages.

comb finger transduction in a typical bias and excitation configuration. The μresonator consists of a shuttle mass, with fingers on opposite sides, suspended 2 μm above a ground plane by folded flexures, which are anchored and shorted to the ground plane at two central points. The shuttle mass is free to move in the direction indicated, parallel to the plane of the silicon substrate. Folding the suspending beams as shown provides two main advantages: first, post-fabrication residual stress is relieved if all beams expand or contract by the same amount; and second, spring stiffening nonlinearity in the suspension is reduced, since the folding truss is free to move in a direction perpendicular to the resonator motion.

The drive and sense capacitors consist of overlap capacitance between the interdigitated shuttle and electrode fingers. As the shuttle moves, these capacitors vary linearly with displacement. Thus, the electrical spring constant, k_e, is ideally nonexistent, and the resonator center frequency is independent of V_P. For actual comb-driven μresonators, nonidealities do not permit absolute cancellation of k_e, and some variation of frequency with V_P is observed. A typically measured frequency variation for a 20 kHz comb-driven μresonator is -54 ppm/°C [1].

Micromechanical Oscillators

The equivalent circuit for the two-port μmechanical resonator of Fig. 4, shown transformed to an equivalent LCR representation, is presented in Fig. 5 [8,9]. Due to the use of weak capacitive electromechanical transduction, the motional element values are quite different from those for quartz crystal units (which typically have R_x=50Ω, C_x=0.04 pF, L_x=0.25 H), and this dictates differing strategies in the design of μresonator oscillators versus macroscopic crystal oscillators. The detailed, transistor-level circuit design and operation of this oscillator has already been discussed elsewhere [2]. The focus of the present discussion centers on issues of amplitude limiting and short-term frequency stability.

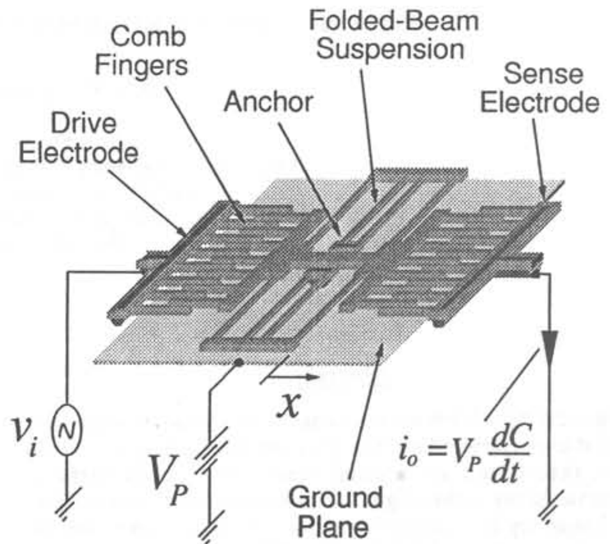

Fig. 4: Perspective view of a two-port, folded-beam, lateral comb-driven resonator with typical applied bias and excitation voltages. All areas of the resonator and electrodes are suspended 2 μm above the substrate, except for the darkly shaded areas, which are the anchor points. The resonator is electrically connected to the ground plane through the anchor points.

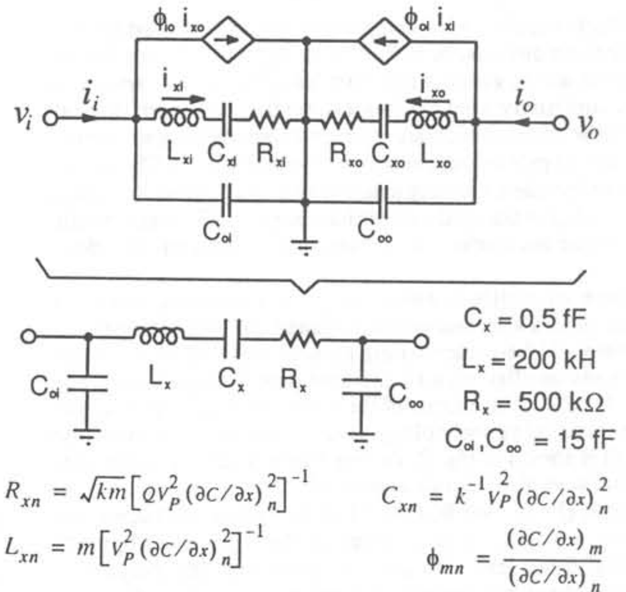

Fig. 5: Equivalent circuit for a two-port μresonator showing the transformation to the more convenient LCR form. In the equations, k is the system spring constant and $(\partial C/\partial x)_n$ is the change in capacitance per displacement at port n of the μresonator.

Amplitude Limiting

Figure 6 shows a system-level schematic describing the basic architecture used for this oscillator. Since the motional resistance of the μresonator is large (Fig. 5), a series resonant oscillator architecture is utilized to minimize Q-loading [2]. As shown, the system consists of a three-port micromechanical resonator, for which two ports are embedded in a positive feedback loop with a sustaining transresistance amplifier, while a third

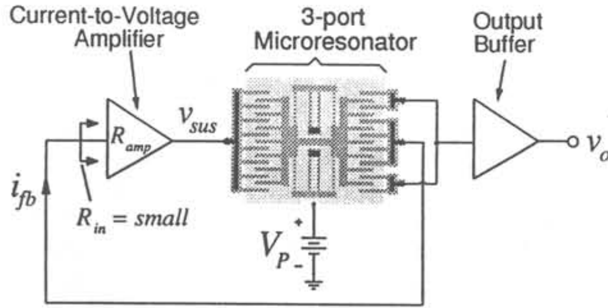

Fig. 6:System level schematic for the μresonator oscillator.

port is directed to an output buffer. The use of a third port effectively isolates the sustaining feedback loop from variations in output loading. Conceptually, the sustaining amplifier and μmechanical resonator comprise negative and positive resistances, respectively. During start-up, the negative resistance of the amplifier R_{amp} is larger in magnitude than the positive resistance of the resonator R_x, and oscillation results. Oscillation builds up until either some form of nonlinearity or a designed automatic-level control circuit alters either or both resistors so that, R_{amp}=R_x, at which point the oscillation amplitude limits.

For oscillators controlled by quartz crystals, the nonlinearity usually appears in the sustaining circuit, where transistors enter the triode region at large voltage amplitudes, reducing effective device transconductances until the loop gain drops to unity. Limiting due to crystal nonlinearity is rare, since quartz crystal units display very little nonlinearity over normal oscillator operating voltage ranges [10].

On the other hand, even though comb-driven, folded-beam μmechanical resonators are only slightly less linear than crystals [2], limiting due to nonlinearity in flexural-mode μresonators is quite practical through adjustment of the dc-bias voltage V_P. As seen from the equations of Fig. 5, the values of the motional circuit elements representing the capacitively driven μmechanical resonator are strongly dependent upon the dc-bias voltage V_P applied to the resonator. In particular, the value of motional resistance R_x is inversely proportional to the square of V_P, and thus, it can be set to just under R_{amp} at the start of oscillation by proper selection of V_P. As oscillation builds up, stiffening nonlinearities in the resonator springs then increase the effective R_x of the μresonator until R_x=R_{amp}, when the loop gain equals one and the amplitude limits. The steady-state amplitude of oscillation is thus a function of the initial separation between R_x and R_{amp}, which is in turn a function of V_P.

Short Term Frequency Stability

In addition to phase noise resulting from superposed electronic amplifier noise, significant noise power contributions are expected from Brownian motion and mass loading [10] of the resonator, since both of these effects become increasingly important as the mass of the resonator element decreases. In particular, the noise component due to Brownian motion is inversely proportional to the square root of resonator mass [1]. The magnitude of mass loading noise depends, not only on resonator mass, but also on the adsorption/desorption rate of contaminant molecules, contaminant molecule size and weight, pressure, and temperature. Theoretical considerations show that mass loading-induced phase noise is maximized at an intermediate value of pressure, but minimized at the low and high pressure extremes [1,10]. Thus, the best phase noise in μmechanical oscillators is achieved at very low pressures, where resonator Q is largest and mass loading noise is smallest. For this reason, vacuum encapsulation strategies [11] which achieve very low pressures may play an important role when using μmechanics for signal processing.

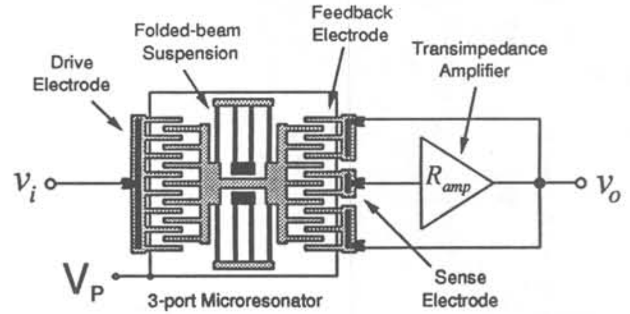

Fig. 7:Circuit schematic for active Q-control for a 3-port μresonator.

Micromechanical Filters

Simple second-order high-Q bandpass filters are often required in communication electronics. A mechanical resonator can provide a high-Q bandpass or lowpass biquad response, depending upon whether resistive or capacitive detection techniques are utilized [12]. A typical measured response for an 18 kHz folded-beam comb-driven μmechanical resonator operated under 20 mTorr pressure yields a quality factor of 50,000, giving an effective -3 dB down bandwidth of 0.36 Hz.

For most practical applications a larger bandwidth is required, so the Q of the resonator must be reduced. Since the initial quality factor of the μmechanical resonator is difficult to predict, any technique used to control Q should be independent of its initial value. One Q-control method which satisfies the above condition and provides ratioed specification of the effective gain of the stage is shown in Fig. 7. Here, a three-port μmechanical resonator is utilized, where an input port accepts an excitation signal, an output port directs resonator motional current to a transresistance amplifier, and a feedback port directs the resulting output voltage back to the resonator. Properly phased competition between the input and feedback ports effectively lowers the Q of the system. The transfer function for the system of Fig. 7 can be written as:

$$\frac{v_o}{v_i}(j\omega) = \frac{N_i}{N_{fb}} \frac{1}{1 + 2jQ'(\Delta\omega/\omega_o)}, \tag{1}$$

where

$$Q' = \frac{[M_{eff}k_{sys}]^{\frac{1}{2}}}{V_P^2 \left(\frac{\partial C}{\partial x}\right)_{fb} \left(\frac{\partial C}{\partial x}\right)_o R_{amp}} \tag{2}$$

is the controlled value of quality factor. In Eq. (1), M_{eff} and k_{sys} are the effective mass and spring constant of the resonator, respectively, and R_{amp} is the transresistance amplification provided by the amplifier. Note that the gain of this stage is completely determined by the ratio of the number of resonator input fingers, N_i, to the number of feedback fingers, N_{fb}, which can be precisely specified to within an error dependent upon the matching tolerance of the $\partial C/\partial x$ for each finger gap. This, combined with Q variability, provides complete freedom in specifying any arbitrary bandpass biquad transfer function via this μelectromechanical system.

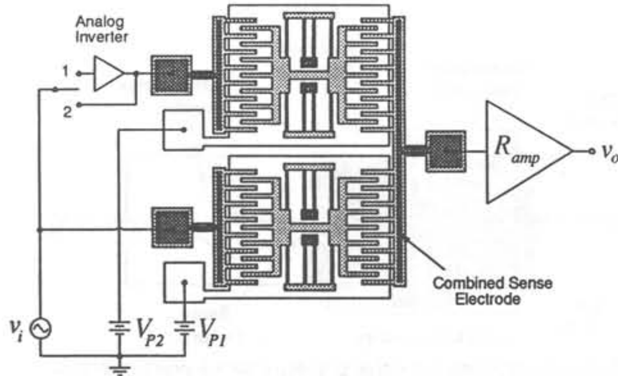

Fig. 8:Schematic of a parallel µresonator filter. When the switch is set at 1, a bandpass filters results; at 2, a notch filter is implemented.

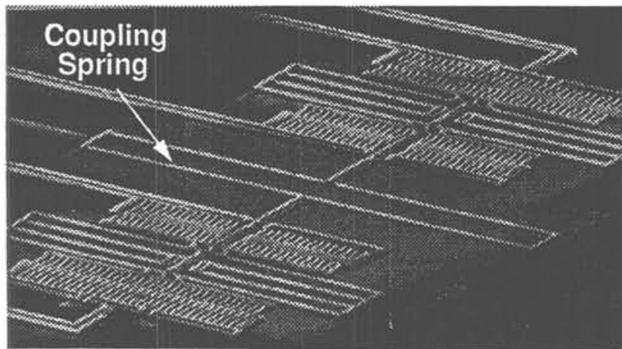

Fig. 9:SEM of a spring-coupled µmechanical filter.

The ability to specify any arbitrary bandpass biquad transfer function makes available a myriad of high order coupled-biquad filter architectures, from cascaded biquad to leap frog [12]. In each of these cases, the minimum bandwidth, temperature dependence, and aging characteristics could be improved when incorporating micromechanical biquads in the design. One simple example of a biquad filter is the parallel electromechanical filter shown in Fig. 8 [13], which consists of two µresonators properly spaced in frequency, with outputs combined to yield a flat passband and steep rolloff outside the passband.

By implementing the coupling, as well as the biquads, mechanically, very compact µmechanical filters can be achieved [13]. One possible design utilizes soft mechanical springs to couple resonators. These filters are designed to match an equivalent electrical LCR ladder filter in the mechanical domain, using either the current or mobility electromechanical analogies. The SEM for a prototype two-resonator µmechanical version of this filter is shown in Fig. 9. The corresponding measured spectrum (using off-chip electronics) is presented in Fig. 10

Conclusions

Completely monolithic, highly stable, high-Q oscillators and electromechanical filters utilizing surface-micromachined polysilicon mechanical resonators have been demonstrated. Due to the novelty of the process and the devices, conservative measures were taken for the designs, and prototypes of up to only 100 kHz were fabricated. Designs up to a few megaHertz are feasible using folded-beam resonator designs, and higher frequencies (tens of MHz) should be feasible using more advanced designs aimed at maximizing resonator quality factor, which

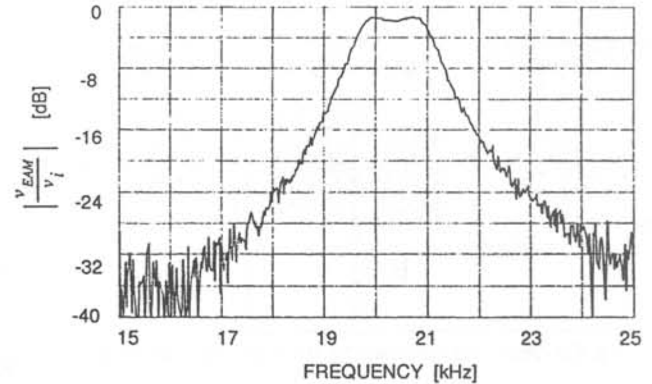

Fig. 10:Measured transfer function for the filter of Fig. 9.

may otherwise degrade with increasing frequency. Both material and architectural improvements should be possible to increase µresonator Q.

Brownian motion and mass loading were identified as phenomena which become increasingly important contributors to phase noise as resonator dimensions shrink. According to theory, mass loading-induced phase noise can be substantially reduced by operating the miniature µmechanical resonator under very low pressures. For this reason, integrated vacuum encapsulation techniques which achieve sub-microTorr pressures may play an important role in the future.

Acknowledgements. The authors would like to thank Shenqing Fang for assistance in CMOS fabrication, as well as Katalin Voros and the staff of the Berkeley Microfabrication Laboratory for process support. In addition, we are grateful for discussions with John Vig of the U.S. Army Electronics Technology and Devices Laboratory, whose insights on mass loading contributed much to this work. This research was supported by the Berkeley Sensor & Actuator Center (BSAC).

References

[1] C. T.-C. Nguyen *et al.*, to be published in the *Proceedings* of the 1994 IEEE International Frequency Control Symposium, 1994.

[2] C. T.-C. Nguyen *et al.*, *IEDM Tech. Digest*, pp. 199-202, 1993.

[3] W. C. Tang *et al.*, *Sensors and Actuators*, **BA21-A23**, pp. 328-331, 1990.

[4] W. Yun *et al.*, *IEEE Solid-State Sensor & Actuator Workshop Tech. Digest*, pp. 126-131, 1992.

[5] C. T.-C. Nguyen *et al.*, *IEDM Tech. Digest*, pp. 505-508, 1922.

[6] C. T.-C. Nguyen *et al.*, *Transducers'93 Tech. Digest*, pp. 1040-1043, 1993.

[7] R. T. Howe *et al.*, *IEEE Trans. Electron Devices*, vol. ED-33, pp. 499-506, 1986.

[8] C. T.-C. Nguyen, M.S. Report, Univ. Calif. Berkeley, 1991.

[9] F. L. Walls *et al.*, *IEEE Trans. Ultrason. Ferroelec. Freq. Contr.*, vol. 39, no. 2, pp. 241-249, March 1992.

[10]Y. K. Yong *et al.*, *IEEE Trans. Ultrason. Ferroelec. Freq. Contr.*, vol. 36, no. 4, pp. 452-458, March 1989.

[11]H. Guckel *et al*, *Sensors and Actuators*, **A21-23**, pp. 346-351, 1990.

[12]C. T.-C. Nguyen, Ph.D. Dissertation, Univ. Calif. Berkeley, to be submitted 1994.

[13]L. Lin *et al.*, *IEEE Micro Electromechanical Systems Workshop Tech. Digest*, pp. 226-231, 1992.